JACS
JOURNAL OF THE AMERICAN CHEMICAL SOCIETY
Article
pubs.acs.org/JACS

Pristine Graphite Oxide

Ayrat Dimiev,[†] Dmitry V. Kosynkin,[†,#] Lawrence B. Alemany,[†,∥] Pavel Chaguine,[†] and James M. Tour*[,†,‡,§,∥]

[†]Department of Chemistry, [‡]Department of Mechanical Engineering and Materials Science, [§]Department of Computer Science, [∥]Smalley Institute for Nanoscale Science and Technology, and [⊥]Shared Equipment Authority, Rice University, MS-222, 6100 Main Street, Houston, Texas 77005, United States

Supporting Information

ABSTRACT: Graphite oxide (GO) is a lamellar substance with an ambiguous structure due to material complexity. Recently published GO-related studies employ only one out of several existing models to interpret the experimental data. Because the models are different, this leads to confusion in understanding the nature of the observed phenomena. Lessening the structural ambiguity would lead to further developments in functionalization and use of GO. Here, we show that the structure and properties of GO depend significantly on the quenching and purification procedures, rather than, as is commonly thought, on the type of graphite used or oxidation protocol. We introduce a new purification protocol that produces a product that we refer to as pristine GO (pGO) in contrast to the commonly known material that we will refer to as conventional GO (cGO). We explain the differences between pGO and cGO by transformations caused by reaction with water. We produce ultraviolet−visible spectroscopic, Fourier transform infrared spectroscopic, solid-state nuclear magnetic resonance spectroscopic, thermogravimetric, and scanning electron microscopic analytical evidence for the structure of pGO. This work provides a new explanation for the acidity of GO solutions and allows us to add critical details to existing GO models.

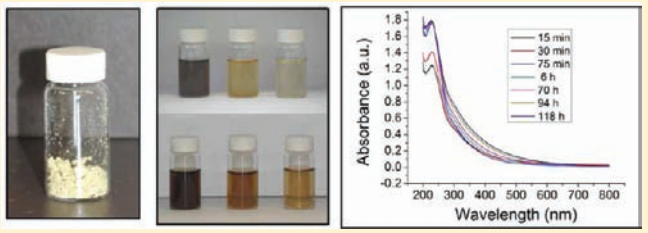

INTRODUCTION

Graphite oxide (GO) has attracted the recurring interest of the chemical community since it was first synthesized in 1855 by Brodie.[1] Numerous studies were done throughout the decades to reveal its structure. Several models of the structure of GO have been developed,[2−9] which often partially exclude each other. The earliest model[2] was developed in 1939, while a more recent model[9] was published in 2006. Despite the effort of many chemists, the structure of GO has remained elusive. In recent years, new interest in GO was sparked after it was found that GO can serve as the precursor for chemically converted graphene (CCG),[10−12] which can be effectively used in fabrication of, for example, transparent conductive films and field effect transistors. GO and its functionalized derivatives have been investigated for applications in optoelectronics, biodevices, drug delivery systems, and composites.[13] One of the interesting properties of GO is its propensity to spontaneously exfoliate in aqueous solutions into monolayer sheets. This is the only known method to readily introduce a monolayer carbon lattice into hydrophilic media.

GO is a lamellar compound, consisting of layers of carbon from the original graphene lattice that have subsequently been oxidized. According to recent studies,[8,9] each single GO layer is considered a multifunctional network, containing several oxygen functionalities in addition to the carbon backbone. The most popular, the Lerf−Klinowski (LK) model,[8] concludes that GO consists of two different randomly distributed domains: (a) pure graphene with sp^2-hybridized carbon atoms and (b) sp^3-hybridized and oxidized carbon domains. In the LK model, the oxidized GO areas contain mostly epoxy and hydroxyl functional groups on the basal planes with carboxyl groups at the edges. Note that Lerf et al. in their work[8] did not obtain any experimental evidence for the presence of carboxyl groups in GO; to the contrary, there was no signal at ∼180 ppm in the ^{13}C NMR spectra of GO, where the carboxyl carbon signal should appear. The conclusion was made on the basis of previously published IR data.[5] However, the absorbance at ∼1730 cm^{-1}, which was interpreted as the C═O bond stretch of the carboxyl groups, can be assigned to any carbonyl group. Thus, today, despite the lack of solid experimental evidence, the presence of carboxyl groups in GO is commonly presumed, and often experimental data are interpreted from the perspective of chemical reactions of carboxyl groups. The Szabo−Dekany (SD) model[9] represents GO as a periodic ribbon-like structure of aromatic and nonaromatic areas. The oxygen functionalities that are thought to be present are hydroxyls and 4-membered ring ethers above and below the plane of the carbon layers. The SD model suggests that ketones and quinones are formed where C−C bonds have been cleaved.

Recent research provides indirect evidence in support of the LK two-domain model.[14−16] Thus, variable temperature electrical measurements of CCG[14] suggest that charge transport occurs via hopping between intact graphene domains of

Received: December 9, 2011
Published: January 11, 2012

   dx.doi.org/10.1021/ja211531y | J. Am. Chem.Soc. 2012, 134, 2815−2822

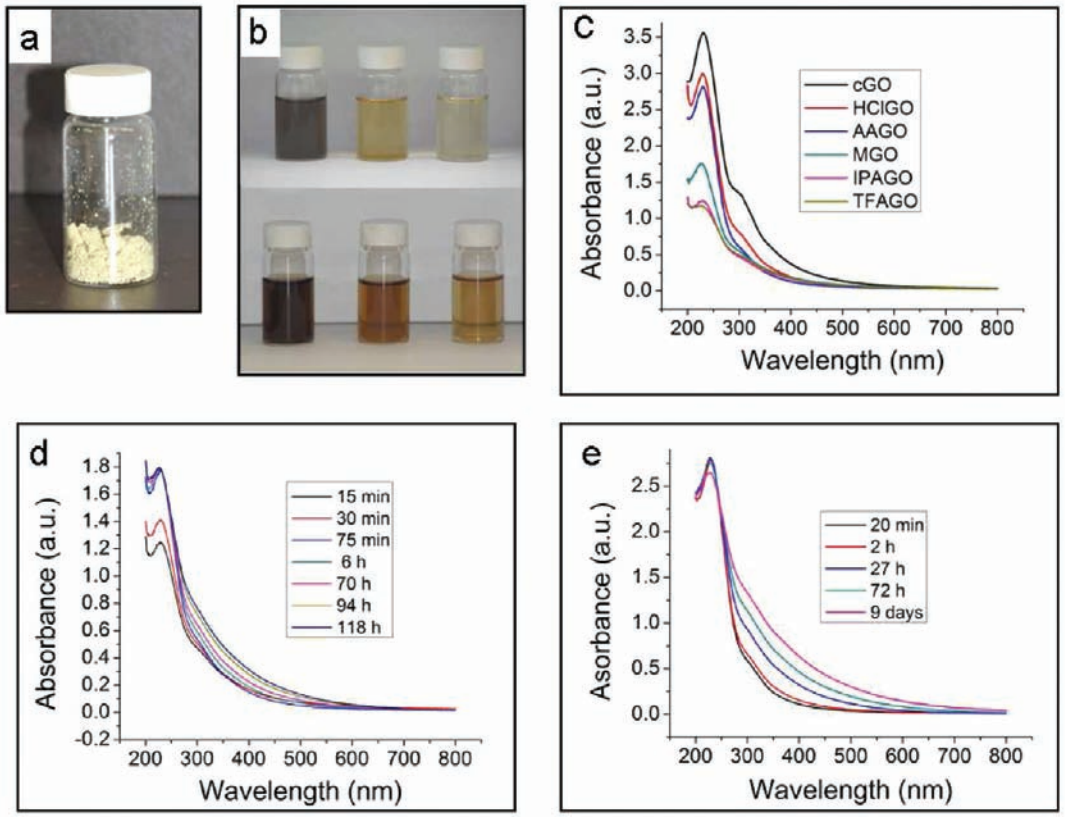

Figure 1. Photographs and UV−vis spectra of the aqueous solutions of the light-colored GO samples. (a) A photograph of dry TFAGO. (b) A photograph of the as-prepared aqueous solutions (top) of the following GO samples (left to right): cGO, MGO, and TFAGO. On the bottom: The same solutions after 24 h. The concentration of the solutions was 0.5 mg/mL. (c) The UV−vis spectra of the aqueous solutions of different GO samples. (d) The change in the UV−vis spectrum of the aqueous IPAGO solution with time. (e) The change in the UV−vis spectrum of the aqueous AAGO solution with time.

nanometer size. A scanning transmission electron microscopy annular dark field (STEM-ADF) image of a GO film[15] revealed strong variations in the ADF intensities, which are uniformly distributed throughout the sheet. Recently, the oxidized and graphene areas of GO were observed by high-resolution transmission electron microscopy (HRTEM).[16]

Despite the fact that the GO lattice was observed at the single-atom level,[16] a more precise chemical structure has not arisen. Accordingly, the reaction pathways that lead to GO are unclear, and the mechanism of GO reduction is also elusive. If we assume that the two different domains suggested by LK do exist, what prevents the oxidation of the aromatic islands in an excess of oxidizing agent? A more precise chemical structure of the oxygenated areas is also unknown.

GO has a high acidity that cannot be explained by any of the existing models. Aqueous solutions of GO have a pH of 3 to 4, and 100 g of GO contains 500−800 mmol[2,4] of active acidic sites that can take part in cation exchange reactions. This is approximately 1 acidic site for every 6−8 carbon atoms. It is unlikely that the small number of carboxylic acid moieties situated on the edges of the GO flake can account for the acidic properties. Clauss and co-workers[4] suggested the presence of enolic groups to explain the observed acidity; however, no experimental support for this suggestion was provided. No other researchers have explained the acidic properties of GO.

The stoichiometric ratio between the constituent elements of GO is not fixed; it varies depending on the level of oxidation. However, this variation is not limitless. Thus, regardless of the preparation method used,[1,17,18] the GO composition and structure do not change significantly with the addition of excess oxidizing agent after achieving some threshold oxidation degree (TOD). Thus, all of the solid-state nuclear magnetic resonance (SSNMR),[6,8,9,19,20] Fourier transform infrared (FTIR) analyses,[6,9,21] and X-ray photoelectron spectroscopy (XPS)[9−12] spectra of the GO products prepared by the three methods are qualitatively similar, suggesting the same set of oxygen-containing functional groups. The C:O ratio for GO samples at TOD prepared by three known methods varies from 1.8 to 2.5, while the most common C:O ratio for different GO samples is ∼2.[2,4−7,9,21] Clauss[4] proposed the ideal empirical formula $C_8O_2(OH)_2$, which despite not being achieved through oxidation, still most adequately reflects the composition of GO. The slight deviations in GO content depend also on the amount of water intercalated between the layers; this water is considered an integral part of any GO. Thus, GO can be defined as a substance that has a constant set of oxygen functional groups (which have not been unambiguously determined) and a narrow range in elemental composition.

In our studies, we discovered that, when using $KMnO_4$ as an oxidizing agent, TOD is achieved after the addition of 4 mass equiv of $KMnO_4$ to a graphite/H_2SO_4 slurry. Therefore, all of the GO samples prepared, modified, and analyzed in this study were made with 4 mass equiv of $KMnO_4$.

In this work, we show that the structure and properties of GO depend significantly on the purification procedures, rather than on the type of graphite used or on the oxidation protocol,

dx.doi.org/10.1021/ja211531y | J. Am. Chem.Soc. 2012, 134, 2815−2822

as is commonly believed.[13] See Table S1 in the Supporting Information for a comparison. We introduce a new purification protocol that produces a product that we refer to as pristine GO (pGO) in contrast to the commonly known material that we will refer to as conventional GO (cGO). The findings allow us to add new details to the GO structure, and thereby propose a refined GO model. The products are characterized by UV−vis, FTIR, ^{13}C SSNMR, thermogravimetric analysis (TGA), and scanning electron microscopy (SEM).

RESULTS AND DISCUSSION

In the two main methods used for GO preparation,[17,18] as well as in their modified versions,[22,23] GO is synthesized in concentrated H_2SO_4, which is known for its high affinity to water. There is little water in the reaction mixture while the graphite is being oxidized, and whatever water is present is protonated as H_3O^+. The first time that the oxidation product is exposed to water is during the quenching and purification steps. To the best of our knowledge, in all of the published work involving the production of GO, the GO was purified by washing with copious amounts of water. GO has a light yellow, almost white color when the reaction mixture is first quenched with water and remains light yellow during the first few aqueous washings. With more washing, the color gradually darkens and changes from yellow to dark brown. This color change suggests significant chemical transformations in the course of purification that result in increased conjugation of the π-system, and thus darkening of the product. On the basis of this color change, the product obtained after washing copiously with water is not identical to the product that was originally produced after the first aqueous quench of the reaction mixture.

To investigate the nature of the as-prepared GO, one needs to avoid exposing the material to water. For this purpose, we conducted a series of experiments where as-prepared GO was quenched and washed by nonaqueous organic solvents capable of dissolving H_2SO_4: methanol (M), glacial acetic acid (AA), trifluoroacetic acid (TFA), ethyl acetate (EA), and isopropanol (IPA). The products produced from quenching and washing by the corresponding solvents are referred to as MGO, AAGO, TFAGO, EAGO, and IPAGO, respectively. In addition, we quenched GO into 10% aqueous HCl where water was present, but the water is significantly protonated and hence less nucleophilic. The resulting product is referred to as HClGO. We will call GO that was quenched and washed with water as conventional GO, or cGO.

Quenching and washing with the listed solvents yielded products with colors that vary from light yellow (Figure 1a) through bright yellow, except the HClGO, which was light-brown. Thus, we use the common name "light-colored GO" for all six listed GO samples: MGO, AAGO, TFAGO, EAGO, IPAGO, and HClGO. On several occasions, we obtained colorless and almost transparent solutions of GO in strong acids. For instance, this was observed upon quenching the reaction mixture of the as-prepared GO into either 85% phosphoric acid or fuming nitric acid in separate experiments, and adding 30% H_2O_2 to convert the purple $KMnO_4$ to colorless K_2SO_4 and $MnSO_4$. The obtained mixtures were completely clear and colorless. These observations along with the light yellow color of TFAGO suggest that the nonaqueous quenched GO lacks sp^2-domains larger than 5 to 6 benzene rings. The five-ringed polycyclic aromatic domains and their derivatives are either colorless or pale-yellow, while all of the six- and seven-ringed structures are deeply colored.[24] Some solid GO samples were bright yellow, indicating absorbance in a narrow region of visible blue light. This suggests that the aromatic domains are of similar size. The brown color is a mixture of different tints. That the water-washed GO is brown is an indication that the sample absorbs in a wide region of the visible spectrum. An increase in the size of the conjugated π-domains, the increase in chromophores in conjugation with these domains, and conjugation of previously isolated π-domains, can all be reasons for the brown color of the products. The chromophores can either develop on the periphery of the domains, from atoms that are a part of the domain, or exist independently and only come into conjugation by virtue of newly formed double bonds connecting them to the domain.

In contrast to water, none of the organic solvents produced pure GO because all of the samples contained 1.2−6.0 atomic % sulfur by XPS analysis. In addition to sulfur, the TFAGO contained Mn (from the $KMnO_4$), while MGO, EAGO, and IPAGO contained K in the form of potassium sulfates. The GO samples quenched and washed with TFA, EA, and IPA contained a significant amount of inorganic contamination, making characterization difficult. To overcome this obstacle, with EA and IPA, the GO was purified in two steps. For those two solvents, the reaction was first quenched in water to remove inorganic K and Mn salts. The nucleophilicity of water in dilute sulfuric acid is greatly reduced by protonation, so its impact on the GO structure is thought to be minimal. At the same time, the inorganic byproduct was soluble in that medium and could be separated from the GO. Thus, a quick acidic water wash was performed to remove the inorganic salts, followed by washings by the corresponding organic solvents to remove sulfuric acid. TFAGO was both quenched in and washed with TFA (see the Supporting Information for details of purification of each GO sample). The dispersibility of the as-prepared light-colored GO samples in the organic solvents and the stability of the prepared dispersions were lower as compared to those of the aqueous colloid solutions. The dispersibility decreased in the sequence: water, 10% aqueous HCl > methanol > acetic acid > ethyl acetate > isopropanol > trifluoroacetic acid.

All of the light-colored GO samples, when dissolved in water, produce light-colored solutions. The solutions slowly darkened with time. Figure 1b (top) shows the as-prepared aqueous solutions of cGO, MGO, and TFAGO. While the cGO solution is dark-brown, the MGO solution is yellow, and the TFAGO solution is almost colorless. Figure 1b (bottom) is a photograph of the same three solutions taken after 24 h. The MGO and TFAGO solutions darkened with time to acquire a brown color, suggesting extension of the conjugated areas. Figure 1c is the UV−vis spectra of the as-prepared aqueous solutions of the six different GO samples at the same concentration taken at near the same time point of dissolution. For the inorganic-contaminated samples, the mass of dissolved GO was increased in accordance with amount of contamination, so the solutions contain equal amounts of GO.

As is evident from Figure 1c, the light-colored GO solutions do not absorb in the 400−800 nm region, consistent with the visual observations. The major difference between the various GO samples is registered in the 200−300 nm region. The cGO spectrum has the characteristic maximum at 230 nm, which is consistent with the literature data.[11] The absorbance in this region is often attributed to conjugated ketones or dienes.[25] Absorbance of the light-colored samples in this region is lower than for cGO, and the peak centered at 230 nm is not as well-pronounced, especially for the MGO, IPAGO, and TFAGO

solutions. The lower absorbance for the light-colored GO samples at 230 nm suggests a lower concentration of the moieties responsible for the absorbance. The absorbance in the 270−350 nm region, which is thought to be due to the conjugated aromatic domains, is also lower for the light-colored GO samples.

Interestingly, for HClGO and AAGO, both of which were quenched into two different acids, the absorbance in the 230 nm region is almost as strong as in cGO, while the absorbance of MGO and IPAGO (washed with the two alcohols) is significantly lower. As is evident from Figures 1d,e, absorbance of the light-colored aqueous solutions increases with time in the broad region 230−700 nm in accordance with the visual observations. However, the change in IPAGO absorbance is different from the change in AAGO absorbance. The absorbance of IPAGO (Figure 1d) at 230 nm significantly increases within the first 75 min of dissolving in water, suggesting the development of functional groups specific to cGO. Because the first scan was performed 15 min after the first contact with water, the absorbance at 230 nm of the sample just after it was exposed to water was probably even lower. After 75 min, absorbance in this region changes little with time, suggesting that development of the functional groups is complete. Absorbance in the 230−700 nm region continues to increase during the following days. Unlike IPAGO (Figure 1d), the functional groups of AAGO (Figure 1e) were already developed. No increase in absorbance with time is measured at 230 nm. After 24 h, the 230 nm peak for the both IPAGO and AAGO slightly flattens, suggesting the change in the nature of the functional groups. The time-dependent increase of absorbance in the 230−700 nm region is more pronounced for AAGO as compared to IPAGO. From the observations, we can conclude that at least two different transformations occur in the as-prepared GO when it reacts with water. The first is the development of oxygen functionalities absorbing at 230 nm, and the second is conjugation of the aromatic domains that absorb in the wide region of 270−700 nm.

FTIR spectra and TGA data for selected light-colored GO samples are provided in Figure 2.

The FTIR spectrum of the cGO is typical for graphite oxide and consistent with the literature data.[6,9,21] The FTIR spectra of the HClGO, MGO, and AAGO (Figure 2a) contain the two enhanced bands at 1417 and 1221 cm^{-1}, which are barely present, if at all, in the cGO spectrum. The intensities of the two bands increase in the order: cGO, HClGO, MGO, and AAGO. The sulfur content of the samples increases in the same order: 0.5%, 1.2%, 2.0%, and 2.6%, respectively, and the two bands at 1417 and 1221 cm^{-1} are consistent with the symmetric and asymmetric stretch of the S=O bond in covalent sulfates.[26,27]

The TGA analysis (Figure 2b) shows that the MGO and IPAGO contain less water. Only 7.5% weight loss is registered in the 21−100 °C temperature interval for both MGO and IPAGO versus 17.8% for the cGO. In the 180−200 °C region, where the cGO loses about 25% of its weight, the MGO and IPAGO lose 14.0% and 17.5% of their weight, respectively. Both MGO and IPAGO exhibit significant weight loss at temperatures above 650 °C, whereas little weight loss is registered for the cGO. Thus, the 18.3% weight loss for the MGO is recorded at 720−770 °C. A 12.7% weight loss is recorded for the IPAGO at 670−730 °C. The TGA data correlate well with the percent sulfur determined by XPS, assuming that the moieties lost contain one sulfur atom for

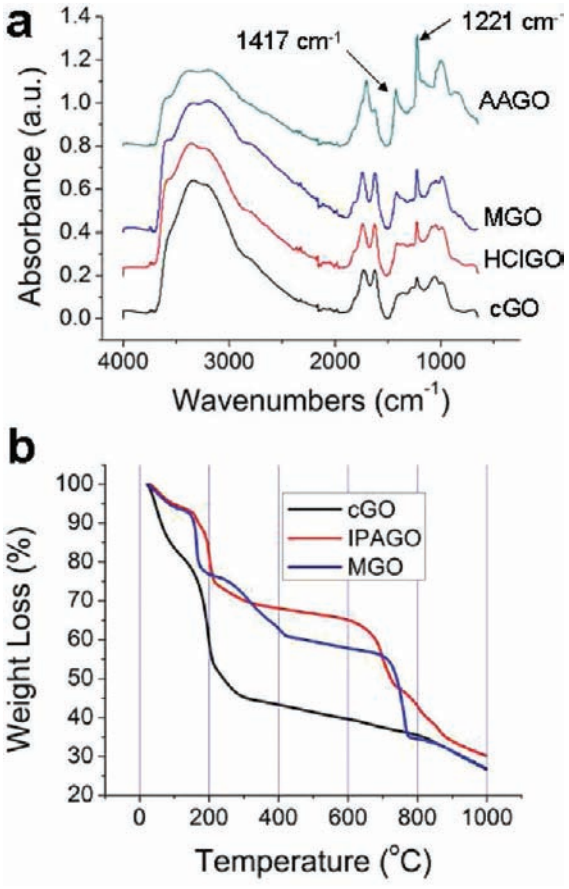

Figure 2. Characteristics of the light-colored GO samples. (a) FTIR spectra of solid AAGO, MGO, HClGO, and cGO samples. The spectra of the remaining three light-colored samples also exhibit strong signals at 1417 and 1221 cm^{-1}, but are significantly affected by the presence of inorganic sulfates. (b) TGA data for the MGO, IPAGO, and cGO.

every four oxygen atoms. According to the XPS data, the samples heated to 400 °C in argon still contain the original amount of sulfur, and the samples heated to 900 °C contain carbon only. Thus, this 640−760 °C weight loss is due to the loss of sulfur.

As was previously discussed, sulfur-containing impurities are difficult to remove using organic solvents. When washing with the most effective solvent, methanol, the sulfur content gradually decreased with the first few washings but did not change after the fifth washing, up to as many as 12 washings. Sulfur-containing impurities are very difficult to remove even by water washing. Thus, all of the water-washed samples contained from 0.5% to 1.0% sulfur. The presence of up to 1.9% sulfur even in the water-washed GO samples was reported earlier.[20,28] It is probable that some amount of sulfur was present in the GO samples for most of studies reported formerly, but it was not determined or it was not reported by the authors. This suggests that the sulfur-containing impurities are covalently bound or strongly physisorbed to GO. Formation of sulfones has been hypothesized.[28] However, sulfones do not absorb at 1417 cm^{-1},[26,27] an absorbance we observe for all of the light-colored GO samples. Only disubstituted covalent sulfates exhibit the absorptions at both 1417 and 1221 cm^{-1}.[26−29] Sulfuric acid and ionic sulfates absorb at different frequencies.

We suggest that covalent sulfates are formed by nucleophilic attack of sulfuric acid or hydrogen sulfate at newly formed epoxides (**1**) in the course of graphite oxidation according to the following reaction (Scheme 1).

Scheme 1. Formation of Covalent Sulfates

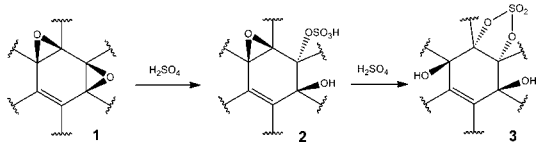

The sulfate ester **2** formed in the first step is the intermediate product. The sulfate ester can attack the neighboring epoxide group resulting in a 1,2-cyclic sulfate **3**. 1,3-Cyclic sulfates (not shown) can be also formed by the reaction. Note that two hydroxyl groups form for every sulfate ester formed.

According to Brimacombe,[29] cyclohexane-*cis*- and *trans*-1,2-diol cyclic sulfates hydrolyze in basic and acidic media. The rate of reaction in acidic conditions, with a half-life of ∼14−16 h, is significantly slower than it is in basic conditions. The first step of the cyclic sulfate hydrolysis occurs with the C−O bond cleavage and results in formation of the monosulfate. Monosulfates are rather stable in basic media but undergo further hydrolysis in acidic solutions, at conditions very similar to those that are present when washing GO with water. The second step (hydrolysis of the monosulfate) occurs mainly with S−O bond cleavage and results in the formation of a 1,2-diol **5** (Scheme 2).

Scheme 2. Hydrolysis of Covalent Sulfates

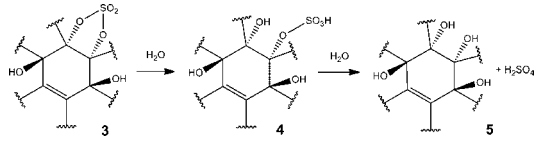

The low rate of sulfate hydrolysis under acidic conditions explains why it is difficult to remove sulfur containing byproduct from a GO sample even when washing with water. Sulfuric acid itself is easily washed away with a few washings, but the covalent sulfates are removed only via hydrolysis, the rate of which is slow under acidic conditions, so that longer reaction times are needed to remove more of those moieties. The second product of the hydrolysis is sulfuric acid, which can be responsible, in part, for the highly acidic properties of GO.

Figure 3 shows SEM images of GO flakes deposited on a Si/SiO_2 wafer by drop-casting of an aqueous EAGO solution. The number of carbon layers can be distinguished by the image opacity.[30] As is evident from Figure 3, the flakes contain different numbers of layers in different areas. The layers are only partially peeled away from each other. This observation suggests the presence of strong interlayer interactions or cross-linking, which holds the two layers together. It has been shown that in aqueous solution GO layers are highly negatively charged,[21] which helps to form stable colloidal solutions. The electrostatic repulsion of the GO layers in aqueous solution is very strong, and the cGO spontaneously exfoliates to monolayer flakes. See Supporting Information Figure 1 for the SEM images of the flakes drop cast from cGO solution. For the EAGO (Figure 3), the interlayer interaction was strong, and the layers were not completely exfoliated. Thus, we suggest that

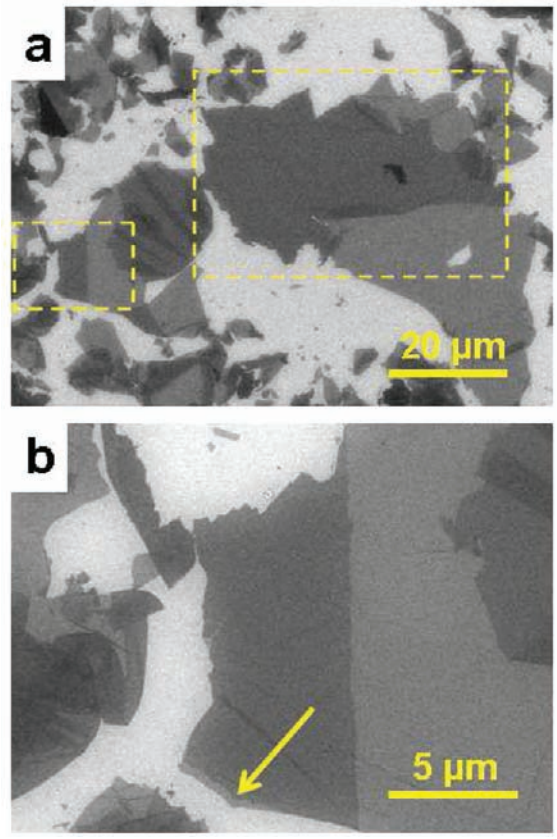

Figure 3. SEM images of GO flakes with partially peeled layers. The flakes are obtained by drop-casting the aqueous EAGO solution (solid EAGO dissolved in water) on the Si/SiO_2 wafer. (a) The low magnification image. The two yellow dash-line rectangles indicate two different GO flakes with partially peeled layers. The contours of the top and the bottom layers coincide, suggesting that these are the two layers of the same flake, not two independent overlapped flakes. (b) A higher magnification image of the smaller yellow-line-contoured rectangular area in (a). The right half of the flake is monolayer, while the left half is bilayer. The yellow arrow points at the area where the top layer is slightly displaced, exposing the bottom layer, and making the wrinkle.

covalent sulfates might exist not only as cyclic sulfates (i.e., bonded to the same carbon layer), but also as bridges between the neighboring layers.

On the basis of our FTIR data (Figure 2a), among all of the solvents tested, water is the most effective in hydrolyzing sulfates. The next most effective is the 10% HCl solution. Apparently, the sulfates are not prone to cleavage in nonaqueous media.

The discussion above is supported by the ^{13}C SSNMR data (Figure 4). The cGO spectrum is typical for graphite oxide and consistent with the literature data.[6,8,9,20,21] The spectra of MGO, EAGO, and IPAGO have similarities to the spectrum of cGO but exhibit a notable difference in the 55−85 ppm region. First, the alcohol signal at 70 ppm is weaker relative to the epoxide signal at 60 ppm (this is not the case for the IPAGO, because it was exposed to a significant amount of water during the first quench). This is expected for a nonaqueous environment. Second, the two peaks are not as well resolved as in the cGO spectrum, which can be explained by the lower alcohol content. Finally, a shoulder emerges in the 75−88 ppm region for the MGO and HClGO, and it is very well

dx.doi.org/10.1021/ja211531y | J. Am. Chem.Soc. 2012, 134, 2815−2822

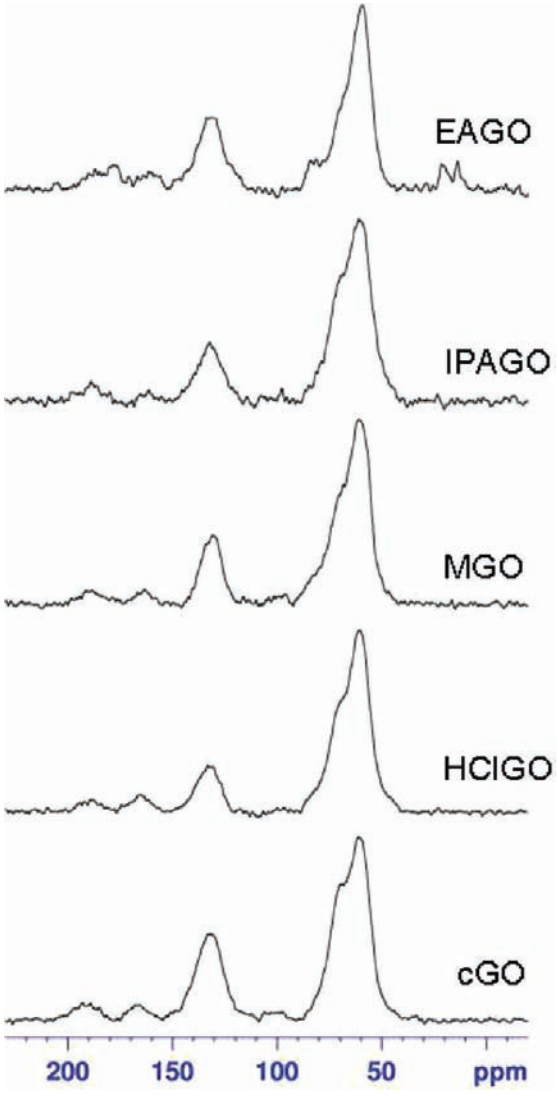

Figure 4. ^{13}C SSNMR spectra of the different GO samples. 50.3 MHz ^{13}C, direct ^{13}C pulse spectra obtained with 12.0 kHz MAS. Expanded plots of just the centerband region are shown. (Plots including spinning sidebands are shown in Supporting Information Figure 2.) The spectra are normalized with respect to the height of the signal at 60 ppm. The weak signals at 14 and 21 ppm in the EAGO spectrum result from residual EA.

pronounced for the EAGO. The calculated chemical shift values for covalent sulfates are located in this region: cyclohexane-1,2-diol cyclic sulfate at 86 ppm, and mono- and disubstituted *tert*-butyl sulfates at 85 and 74 ppm, respectively.[31] Interestingly, the spectrum of HClGO is markedly different from the spectrum of cGO. The relative intensity of the sp^2-carbon signal at 134 ppm is significantly lower on the HClGO spectrum (14.5%) as compared to that of the cGO spectrum (26.4%). It is also lower than in the spectra of MGO (18.0%), IPAGO (17.5%), or EAGO (21.9%). Thus, washing with aqueous HCl is the unique case, where the sulfates are cleaved, but the high acidity does not lead to the extension of conjugation.

As it is apparent from discussions above, the light-colored GO differs from the dark-brown cGO both by composition and by physical properties. We refer to light-colored GO as pGO in contrast with the material normally obtained by researchers after extensive washings with water, cGO. The cGO is the product of reaction between pGO and water. As an analogy, as the oxide SO_3 reacts with water to form sulfuric acid, so the oxide pGO reacts with water to form cGO. "Graphitic acid", the term by which graphite oxide was referred by many researchers in the past,[3,17] may be the more descriptive method of naming the material.

The reaction of GO with water leads to an increase of the sp^2-carbon content as evident from the ^{13}C SSNMR spectra (Figure 4). The reaction is triggered by hydrolysis of covalent sulfates, which serve as protective groups. The content of the C═C is lower in compounds not exposed to water (MGO, EAGO) and exposed to highly protonated water (HClGO). This observation suggests that the nature of the reaction is nucleophilic attack by water or due to the basicity of water.

On the basis of the data discussed, we propose the further GO transformations that occur during washing with water, after the sulfates have been cleaved resulting in formation of 1,2-diols (Scheme 3).

Scheme 3. GO Transformations Caused by Reaction with Water[a]

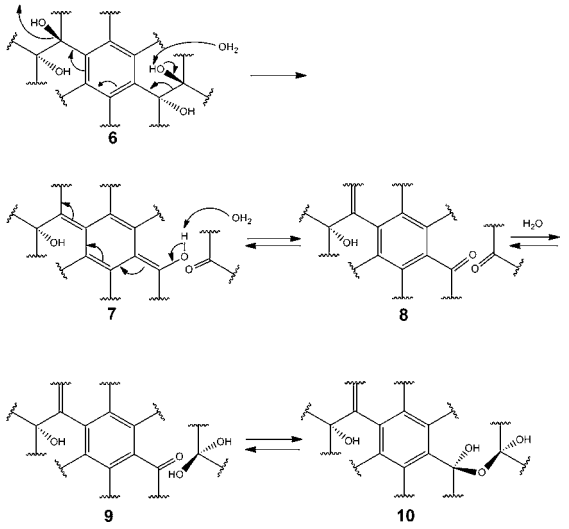

[a]Double bonds form at the expense of tertiary alcohols and C−C bond rupturing.

Structure **6** is the GO fragment containing a 1,2-diol that was formed after opening of an epoxide or the cleavage of a cyclic sulfate (Scheme 2). One out of the two hydroxyl groups ionizes and results in cleavage of the C−C bond with formation of ketone and enol **7**. These steps are accompanied by elimination of one hydroxyl group and formation of one additional C═C bond resulting in the extension of the conjugated area. The enol in the structure **7** can ionize with simultaneous formation of one more double bond to form **8**. The conjugated hydroxyl group shown in **7** could be part of a vinylogous carboxylic acid, thereby lowering its pK_a enough to be deprotonated in water. The resulting conjugate base is stabilized by delocalization of the negative charge over the large conjugated sp^2 area. We mentioned above that the graphite oxide flakes in aqueous solution are highly negatively charged. Thus, the suggested reaction mechanism explains two experimental observations: the extension of conjugated areas, and the GO acidic properties by stepwise conversion of tertiary alcohols into ketones. The conjugated area is extended at the expense of tertiary alcohols. As compared to **6**, **8** contains one additional C═C bond and

dx.doi.org/10.1021/ja211531y | *J. Am. Chem.Soc.* 2012, 134, 2815−2822

two carbonyls, both conjugated with sp^2-carbon domains. The conjugated carbonyl is a strong chromophore. The ketone peak at 189 ppm is larger on the cGO NMR spectrum as compared to that in the HClGO spectrum (4.5% and 3.4%, respectively, out of the total carbon content), which supports the suggested reaction. However, the increase in the ketone content is not as significant as the increase in C=C carbon content (26.4% and 14.5%, respectively). This observation suggests that the ketones in **8** might undergo further transformation. One of the possible ways is hydration and conversion into gem-diols such as **9**. Gem-diols are stable at reaction conditions, especially when carbonyls or double bonds are present in the α-position to the gem-diol carbon and the strain favors sp^3-hybridization.[32,33] There is another possible transformation in that **9** can be further converted to **10** by formation of hemiacetals. Both **9** and **10** contain a sp^3-carbon atom bonded to two oxygen atoms, which might be responsible for the 101 ppm shift in the ^{13}C SSNMR spectrum of cGO.

According to the most popular GO model,[8] the flake edges are terminated by carboxyl groups. Considering the average GO flake size in our samples (Supporting Information Figure S1), the ratio of the edge carbon atoms to the basal plane atoms is ~1/10 000. Such a small number of edge carbon atoms cannot be responsible for the high content of C=O atoms both in the literature data[6,8,20,21] and in our data (Figure 4). The combined content of the carbonyl carbon atoms was 9.5% in ref 20 and 7.6% based on our experimental data for cGO. Therefore, most of the C=O atoms are located within the basal planes or, more exactly, on the edges of the vacancy defects in the basal planes. On the basis of the content of C=O functional groups, there is approximately one edge carbon atom per every 10–12 carbon atoms of the lattice. Because all of the light-colored GO samples already contain carbonyl groups (Figures 2a and 4) and their content is not significantly lower in comparison to cGO, it should be assumed that pGO already contains vacancy defects as it is produced from graphite.

Importantly, it was further discovered that a gas was produced in the course of the oxidation of graphite. In one of the experiments, oxidation of graphite (8.00 g) yielded CO_2 (290 mL), identified by gas chromatography, with more intense production at the end of the reaction. Transferring the evolved gas through a $Ba(OH)_2$ solution yielded $BaCO_3$, identified by FTIR. In this experiment, each 55 carbon atoms yielded 1 CO_2. In another experiment, oxidation of graphite (6.00 g) yielded CO_2 (340 mL), which is 1 CO_2 for every 35 carbon atoms. Apparently, the graphite oxidation reaction that takes place at the solid–liquid graphite–sulfuric acid interface is diffusion controlled and therefore yields different data. Thus, the vacancy defects form in the course of GO production. This is a possible explanation for why CCG cannot be restored to its full graphene-like electronic properties.[14,34] We suggest that the ketones that terminate the large vacancy defects are significantly hydrated.

CONCLUSIONS

As-prepared GO was quenched and washed by nonaqueous solvents, and the corresponding products were characterized. The pGO, as it was produced by oxidation of graphite, contains a significant amount of vacancy defects terminated by ketone groups. The size of aromatic domains does not exceed 5–6 benzene rings. Oxidized sp^3 areas are dominated by epoxides. Covalent sulfates and alcohols are present in smaller amounts. The neighboring carbon layers might be cross-linked by covalent sulfates.

The cGO is the product of numerous chemical transformations, which occur when the pGO is exposed to water. These transformations are responsible for the acidic properties of GO that can be explained by stepwise conversion of tertiary alcohols into ketones, where the electrons lost by the ionized hydrogen atoms are used to extend the conjugated areas. The ketones that terminate the large vacancy defects are in equilibrium with their hydrated forms. The acidic properties of GO samples can be also explained by the presence of incompletely hydrolyzed covalent sulfates. Although we have proposed an updated GO model and explained its high acidity without referring to carboxyl groups, we cannot rule out their presence in GO.

ASSOCIATED CONTENT

Supporting Information

Methods, additional characterization, comparison Table S1, and SEM and NMR data. This material is available free of charge via the Internet at http://pubs.acs.org.

AUTHOR INFORMATION

Corresponding Author

tour@rice.edu

Present Address

[#]Saudi Arabian Oil Company, Dhahran 31311, Saudi Arabia.

ACKNOWLEDGMENTS

This work was funded by the AFOSR (FA9550-09-1-0581), the AFRL through University Technology Corp. (09-S568-064-01-C1), the Office of Naval Research Graphene MURI Program (00006766, N00014-09-1-1066), and M-I SWACO, LLC.

REFERENCES

(1) Brodie, B. *Ann. Chim. Phys.* **1855**, *45*, 351–353.
(2) Hofman, U.; Holst, R. *Ber. Dtsch. Chem. Ges.* **1939**, *72*, 754–771.
(3) Ruess, G. *Monatsh. Chem.* **1947**, *76*, 381–417.
(4) Clauss, A.; Plass, R.; Boehm, H.-P.; Hofmann, U. *Z. Anorg. Allg. Chem.* **1957**, *291*, 205–220.
(5) Scholz, W.; Boehm, H.-P. *Z. Anorg. Allg. Chem.* **1969**, *369*, 327–340.
(6) Mermoux, M.; Chabre, Y.; Rousseau, A. *Carbon* **1991**, *29*, 469–474.
(7) Nakajima, T.; Mabuchi, A.; Hagiwara, R. *Carbon* **1988**, *26*, 357–361.
(8) Lerf, A.; He, H.; Forster, M.; Klinowski, J. *J. Phys. Chem.* **1988**, *102*, 4477–4482.
(9) Szabo, T.; Berkesi, Ot.; Forgo, P.; Josepovits, K.; Sanakis, Y.; Petridis, D.; Dekany, I. *Chem. Mater.* **2006**, *18*, 2740–2749.
(10) Stankovich, S.; Dikin, D. A.; Piner, a. R. D.; Kohlhaas, K. A.; Kleinhammes, A.; Jia, Y.; Wu, Y.; Nguyen, S. T.; Ruoff, R. *Carbon* **2007**, *45*, 1558–1565.
(11) Li, D.; Muller, M.; Gilje, S.; Kaner, R.; Wallace, G. *Nat. Nanotechnol.* **2008**, *3*, 101–105.
(12) Tang, V.; Allen, M.; Yang, Y.; Kaner, R. *Nat. Nanotechnol.* **2009**, *4*, 25–29.
(13) Dreyer, D. R.; Park, S.; Bielawski, W.; Ruoff, R. S. *Chem. Soc. Rev.* **2010**, *39*, 228–240.
(14) Gomez-Navarro, C.; Weitz, R.; Bittner, A.; Scolari, M.; Mews, A.; Burghard, M.; Kern, K. *Nano Lett.* **2007**, *7*, 3499–3503.
(15) Mkhoyan, K. A.; Contryman, A. W.; Silcox, J.; Stewart, D. A.; Eda, G.; Mattevi, C.; Miller, S.; Chhowalla, M. *Nano Lett.* **2009**, *9*, 1058–1063.

(16) Erickson, K.; Erni, R.; Zonghoon Lee, Z.; Alem, N.; Will Gannett, A.; Zettl, A. *Adv. Mater.* **2010**, *22*, 4467−4472.
(17) Staudenmaier, L. *Ber. Dtsch. Chem. Ges.* **1898**, *31*, 1481−1487.
(18) Hummers, W. S.; Offeman, R. E. *J. Am. Chem. Soc.* **1958**, *80*, 1339.
(19) Cai, W.; Piner, R. D.; Stadermann, F. J.; Park, S.; Shaibat, M. A.; Ishii, Y.; Yang, D.; Velamakanni, A.; An, S. J.; Stoller, M.; An, J.; Chen, D.; Ruoff, R. S. *Science* **2008**, *321*, 1815−1817.
(20) Gao, W.; Alemany, L. B.; Ci, L.; Ajayan, P. M. *Nat. Chem.* **2009**, *1*, 403−408.
(21) Szabo, T.; Tombacz, E.; Illes, E.; Dekany, I. *Carbon* **2006**, *44*, 537−545.
(22) Kovtyukhova, N. I.; Olliver, P. J.; Martin, B. R.; Mallouk, T. E.; Chizhik, S. A.; Buzaneva, E. V.; Gorchinskiy, A. D. *Chem. Mater.* **1999**, *11*, 771−778.
(23) Marcano, D. C.; Kosynkin, D. V.; Berlin, J. M.; Sinitskii, A.; Sun, Z.; Slesarev, A.; Alemany, L. B.; Lu, W.; Tour, J. M. *ACS Nano* **2010**, *4*, 4806−4814.
(24) Harvey, R. A. *Polycyclic Aromatic Hydrocarbons*; Wiley-VCH: New York, 1997.
(25) Pavia, D. L.; Lampman, G. M.; Kriz, G. S. *Introduction to Spectroscopy: A Guide for Students of Organic Chemistry*; Saunders College Publishing: Philadelphia, PA, 1979.
(26) Grasselli, J. G. *Atlas of Spectral Data and Physical Constants for Organic Compounds*; CRC Press: Cleveland, OH, 1973.
(27) Kharasch, N. *Organic Sulfur Compounds*; Pergamon Press: New York/Oxford/London/Paris, 1961.
(28) Petit, C.; Seredych, M.; Bandosz, T. J. *J. Mater. Chem.* **2009**, *19*, 9176−9185.
(29) Brimacombe, J. S.; Foster, A. B.; Hancock, E. B.; Overend, W. G.; Stacey, M. *J. Chem. Soc.* **1960**, 201−211.
(30) Dimiev, A.; Kosynkin, D. V.; Sinitskii, A.; Slesarev, A.; Sun, Z.; Tour, J. M. *Science* **2011**, *331*, 1168−1172.
(31) Predicted NMR data calculated using Advanced Chemistry Development Inc. software V11.01 ACD/Labs.
(32) Shapiro, Y. M. *Russ. Chem. Rev.* **1991**, *60*, 1035−1049.
(33) Krois, D.; Langer, E.; Lehner, H. *Tetrahedron* **1980**, *36*, 1345−1351.
(34) Sinitskii, A.; Dimiev, A.; Kosynkin, D. V.; Tour, J. M. *ACS Nano* **2010**, *4*, 5405−5413.